HHS Public Access

Author manuscript

World Neurosurg. Author manuscript; available in PMC 2024 May 06.

Published in final edited form as:

World Neurosurg. 2017 October ; 106: 120–130. doi:10.1016/j.wneu.2017.06.128.

Intraoperative Near-Infrared Optical Contrast Can Localize Brain Metastases

John Y. K. Lee, MD, MSCE[1], **John T. Pierce, MS**[1], **Ryan Zeh, BA**[1], **Steve Cho, BS**[1], **Ryan Salinas, MD**[1], **Shuming Nie, PhD**[3], **Sunil Singhal, MD**[2]

[1]Department of Neurosurgery, Hospital of the University of Pennsylvania

[2]Department of Surgery, Hospital of the University of Pennsylvania

[3]Department of Biochemistry, Emory University

Abstract

Introduction: Approximately 100,000 brain metastases are diagnosed annually in the United States. Our lab has pioneered a novel technique, “Second Window Indocyanine Green (SWIG)”, which allows for real-time intraoperative visualization of brain metastasis through normal brain parenchyma and intact dura.

Methods: Thirteen patients with intraparenchymal brain metastases were administered indocyanine green (ICG) at 5mg/kg the day prior to surgery. A Near-Infrared capable camera was used intraoperatively to identify the tumor and to inspect surgical margins. Neuropathology was used to assess the accuracy and precision of the fluorescent dye for identifying tumor.

Results: ICG was infused at 24.7 ± 3.45 hours before visualization. All thirteen metastases fluoresced with an average signal-to-background ratio (SBR) of 6.62. The SBR with the dura intact was 67.2% of the mean SBR once the dura was removed. The NIR signal could be visualized through normal brain parenchyma up to 7 mm. For the 39 total specimens, the mean SBR for tumor specimens (n=28) was 6.9 whereas the SBR for non-tumor specimens (n=11) was 3.7. The sensitivity, specificity, PPV and NPV of NIR imaging for tumor was 96.4%, 27.3%, 77.1%, and 75.0%.

Discussion: SWIG relies on the passive accumulation of dye in abnormal tumor tissue via the enhanced permeability and retention (EPR) effect. It provides strong NIR signal-to-background ratio which can be utilized to localize tumors prior to dural opening. The use of SWIG for margin assessment remains limited by its lack of specificity (high false positive rate); however, ongoing improvements in imaging parameters show great potential to reduce false positives.

Corresponding Author: John Y K Lee, MD, leejohn@uphs.upenn.edu, Department of Neurosurgery, University of Pennsylvania, 235 South Eighth Street, Philadelphia, PA 19107.

Conflict of Interest: JYKL owns stock options in VisionSenseTM.

Keywords

fluorescence; brain tumor; indocyanine green; second window ICG; near-infrared

Introduction

Metastatic brain tumors are among the most common type of brain tumor. Approximately 100,000 people are diagnosed with brain metastases in the United States each year, and an estimated 24–45% of all patients with solid tumors in the United States develop a brain metastasis[22]. Surgical resection remains a primary treatment strategy. However, despite maximal safe surgical resection of brain metastasis, local recurrence can still be as high as 50% without adjunct radiation[23].

In order to reduce the local recurrence rate, multiple intraoperative imaging technologies such as fluorescence imaging have been explored to delineate tumor margins and to improve gross total resection. The most commonly used contrast agent for intraoperative brain tumor imaging has been 5-aminolevulinic acid (5-ALA)[31]. Specifically, it has been utilized to reduce recurrences after glioblastoma surgery. 5-ALA is a pro-drug in the porphyrin family that has been trialed extensively in Europe and Asia but is not FDA approved for use in the United States[3,4,31,32,34,35,37].

Our lab has been studying another contrast agent, and we have developed a novel technique termed “Second Window ICG (SWIG)” which allows for real time intraoperative visualization of brain tumors and provides for visualization of tumor dye through normal brain parenchyma and intact dura[13,14].

Indocyanine Green has been used for many decades as a vascular contrast agent. Its primary role has been a fluorescent dye for video angiography[6,11,18,28]. Our lab has developed a novel technique to infuse indocyanine green at 5 mg/kg up to 24 hours prior to surgery[12,26,27]. This novel imaging strategy utilizes the enhanced permeability and retention (EPR) effect to concentrate ICG to the tumor[1,6,7,8,9,15,16,17]. We have previously reported our experience in gliomas, and we identified that only gadolinium-enhancing gliomas appear to fluoresce using the SWIG technique[14]. In this study, we hypothesized that Second Window ICG could localize brain metastases in situ in real time in the operating room, and could be used to identify margins intraoperatively.

Methods

Study Design

This is a prospective cohort study that was approved by the University of Pennsylvania Institutional Review Board, and all patients gave informed consent. The trial is registered under clinicaltrials.gov with identifier NCT02710240, and recruitment commenced in October 2014. Any adult patient (age 18 years and greater) undergoing craniotomy for brain tumor was considered eligible for this study. Pregnant woman and an allergy to iodide or shellfish were the main exclusion criterion. All patients underwent preoperative magnetic resonance imaging (MRI) of the brain with intravenous gadolinium. The presence or absence

of gadolinium enhancement, tumor size, fluid-attenuated inversion recovery (FLAIR) and mass effect on MR imaging were noted. MRI image analysis was performed using GE PACS software. FLAIR signal was classified as none, mild or significant (significant being more than twice the size of the lesion). Patients were consented and informed that the scope of surgery would not substantially change based on NIR findings, and biopsies would be taken only if deemed safe by the senior neurosurgeon (JYKL).

NIR Imaging Contrast Agent

Patients were infused intravenously with a 5 mg/kg dose of indocyanine green (C43H47N2O6S2.Na) (Akorn Pharmaceuticals, IL). 25mg vials of ICG were reconstituted with 10 mL of distilled water provided with the packaging. The calculated dose volume was emptied into a 250 mL intravenous bag and distilled water was then added to bring the total volume to 250mL. Note that this formulation is an off-label use of the ICG, and as such all patients were enrolled in IRB-approved study. Patients were infused the day prior to surgery based on preclinical and clinical studies from our laboratory[13,14.29,30].

NIR Imaging System

All cases were imaged using the VisionSense Iridium™ camera system (VisionSense, Philadelphia, PA). This system is FDA-approved for perfusion imaging in plastic and reconstructive surgery (e.g. to assess for flap viability)[25]. The excitation source was a NIR laser (805nm). An algorithm created a heat map displaying visible signal overlaid on fluorescence signals. Image processing is done in real time and presented at 1080p video resolution (with recording at 720p). Its sensitivity to ICG is high and is in the picomolar range for IRDYE800, a similar NIR contrast agent[5].

Study Procedures

Patients underwent anesthesia and a craniotomy using anatomic landmarks as well as neuronavigational imaging. Preoperative MRI was used for navigation in all subjects. All preoperative MRI data were performed on either a 1.5 or 3T scanner using Gabobenate Dimeglumine 529mg/ml contrast agent with boluses ranging from 8 to 20mL. The craniotomy was performed as standard-of-care. All patients received 0.5 mg/kg intravenous mannitol prior to dural incision. Most patients were already on dexamethasone at various doses prior to surgery as prescribed by their oncologist. All patients were administered intravenous leveritacem loading dose for the surgery.

Upon dural exposure, the operating room lights were dimmed, and the NIR imaging system was sterilely draped and positioned above the operative field. The presence or absence of NIR signal was documented post-hoc and recorded in binary yes/no format. This was referred to as the DURA view. The dura was then opened, and the camera was brought into the field, and the ability to localize NIR signal corresponding to the tumor prior to cortical incision, CORTEX view, was also recorded in binary yes/no format. For the tumors deep to the cortex, the depth was noted on preoperative MRI and the presence of a clear NIR signal was recorded in a binary yes/no format in order to determine depth of visualization. Surgery then proceeded in the standard manner without the use of NIR-imaging adjuncts. For tumors

deep to the cortex, after performing the corticectomy, the camera was brought in again and an additional attempt was made at the time of tumor identification, TUMOR view.

When the attending neurosurgeon was satisfied that a complete resection had been achieved, NIR-imaging was used to identify areas of residual disease, referred to as the MARGIN view. A complete resection based on visible light imaging was performed prior to bringing in the NIR camera for margin visualization. The surgeon's impression of the tumor itself and the margin biopsy samples were recorded in binary format as well as photo documented for post-hoc analysis. Areas were biopsied at the discretion of the senior neurosurgeon (JYKL). All margin specimens were taken directly from the adjacent parenchyma. No margins were taken from more distant locations. Of note, the camera exposure settings were not controlled, and thus a dynamic auto-exposure was employed throughout. This allowed us to optimize our sensitivity for identifying small quantities of disease.

During surgery, all specimens were coded by the attending neurosurgeon (JYKL) as consistent with tumor with bright light (white: yes/no) and with NIR-fluorescence (NIR: yes/no). The histopathologic diagnosis obtained several days later served as the gold standard and was catalogued by the Neuropathologists at our institution. The presence of tumor, gliosis, atypical cells, necrosis or inflammation were noted and incorporated into our analysis.

Patients were admitted to the intensive care unit following surgery. There were no adverse outcomes. An MRI took place on the first post-operative day. Patients were seen at approximately two and four weeks after surgery in the neurosurgery clinic.

Data Analysis

The data from the thirteen patients was analyzed using SPSS™ and STATA 10™. To quantitate the amount of fluorescence from the tissue, we used region-of-interest (ROI) analyses within the VisionSense software (VSPlayer v1.8.05.01). In addition, a background reading was taken from adjacent normal surrounding dura or brain tissue. Together, the signal-to-background ratio (SBR) was generated from dividing the mean tumor fluorescence as a proportion of the normal brain parenchyma fluorescence. MRI image analysis was performed using GE® PACS software. Region-of-interest (ROI) analysis was performed on approximate area of 1cm diameter circles on axial T1 post-contrast studies. An ROI was drawn in the tumor as well as in the adjacent normal brain parenchyma in order to calculate a T1 post-contrast tumor to non-tumor signal ratio. Two-by-two contingency tables were constructed using SPSS™ and STATA 10™, and sensitivity/specificity/receiver operating characteristic (ROC) analysis were calculated to assist in interpretation of the data. P-values of 0.05 and less were considered statistically significant. By calculating the area under the curve generated by plotting true positive (y) versus false positive (x) rates, we could determine the test discrimination—which reflects the ability of the test to properly classify those without and those with the disease.

Results

Second Window ICG causes fluorescence of metastatic tumors to the brain

Between November 2014 and May 2016, 13 patients (n=4 male) between the ages of 36 and 73 (mean 59) with a diagnosis of brain metastasis were enrolled (Table 1: Description of Patients – Demographics & Infusion parameters). The 13 subjects presented with a wide array of disease pathology: 4 primary lung metastases, 2 melanoma, 2 colon, 2 breast, 1 ovarian, 1 kidney, and 1 esophageal metastasis. Subject BMIs ranged from 17.94 to 33.8 (mean 26.15). Overall survival using Kaplan-Meier analysis was 271 days

Preoperative T1 and T2 weighed MRI scan demonstrated intraparenchymal metastasis with a diameter ranging from 16.1mm – 44.3mm (mean 25.8 mm) (Table 2: MRI and Near-Infrared Signal of Gross Tumor Specimen). 8 tumors were located on the right side and 5 on the left side of the midline. On preoperative MRI, 4 (31%) tumors showed significant flair, 7 (54%) showed mild flair and 2 (15%) showed no flair abnormality. In addition, the intensity of T1 gadolinium enhancement was calculated by drawing an ROI over the tumor and comparing to adjacent uninvolved brain parenchyma.

Typically, ICG is used to image vasculature as an angiography technique usually within a few minutes of injection. The half-life of ICG within circulation is only a few minutes. Thus, in order to determine if our technique with Second Window ICG would be effective for brain tumors, all patients underwent preoperative infusion the day prior to surgery. Of the thirteen patients, one patient experienced an episode of transient hypoxia to 89% oxygen saturation following the infusion which recovered without specific intervention within minutes. This patient had prior lung cancer lobectomy and radiation fibrosis as well as cardiac comorbidities which predisposed him to hypoxia. No specific interventions were undertaken, as his oxygen saturation recovered spontaneously within minutes.

During surgery, all thirteen metastasis demonstrated strong signal-to-background ratio (SBR 6.62 ± 1.6) (Table 2: MRI and Near-Infrared Signal of Gross Tumor Specimen). We tested several hypotheses to identify factors that may influence the intensity of the fluorescent signal. Previously, we found a correlation between T1 contrast enhancement and the brightness of the signal, but in this case, the intensity of T1 contrast enhancement did not correlate with SBR (R-squared = 0.0064)[13].

One of the patients in this series had a hemorrhagic melanoma metastasis which was primarily cystic with an obscured mural nodule. The melanin/blood did not show any fluorescence, but upon evacuating the cyst contents, the presumed contrast-enhancing mural nodule showed strong SBR (Figure 2). Overall, however, melanoma metastasis appeared to have the weakest SBR (SBR=3.65 for two melanoma metastases versus SBR = 7.2 for the 11 other metastases) which may be related to melanin’s ability to block light penetration (Table 2).

Second Window ICG allows visualization of deep brain metastases

Near-infrared light possesses a longer wavelength than visible light, and thus tissue penetration is greater than visible light. We hypothesized that we would be able to visualize NIR signal through brain parenchyma and potentially through the dura as well.

First, we performed NIR imaging prior to dural opening – DURA view (n=11), prior to corticectomy – CORTEX view (n=7), at initial exposure of tumor – TUMOR view (n=13), and after conventional gross total resection – MARGIN view (n=13). The SBR of the 11 patients with DURA view was 4.42 ± 1.5 (Figure 1 and 3: SBR at Dura, Cortex and Tumor). After the dura was opened and reflected away from the cortical surface, the SBR increased to 5.67 ± 1.1 compared to 4.42 ± 1.5 with the dura intact. Upon exposure of the tumor itself via corticectomy, the SBR increased to 6.62 ± 1.6. Hence, the SBR before dural opening was 67% of final SBR, and the SBR through the intact brain parenchyma was 86% of the final SBR once the metastasis was exposed and visualized. These differences were not significant using ANOVA between the three groups (P=0.2126) most likely because of few numbers.

Second, to determine the maximum depth of visualization of NIR through normal brain parenchyma, we focused on the metastasis that had no visible changes to the surface of the brain (n=5). These 5 metastases ranged from 2.7mm to 29.3 mm from the surface of the cortex to the outer most edge of the tumor based on T1-weighted MRI. The tumor at 29.3mm could not be seen with our NIR camera system. The four other deep tumors (2.7, 2.9 6.0, and 6.8mm) all four displayed a strong NIR signal which allowed for localization of the tumor prior to making the durotomy. The SBR for these four deep tumors through the dura was 4.6 ± 1.1. The SBR for these four deep tumors when the dura was resected back and the cortex was exposed was 5.2 ± 0.6, and the final SBR at exposure of tumor SBR was 6.14 ± 3.0.

Margin Identification - Test Characteristics of Visible versus NIR imaging.

After tumor identification, the tumor was resected in a standard manner, and the NIR camera was brought into the field to inspect and biopsy the margins. Choice of site of margin biopsy was based on presence of NIR signal. Only margins deemed safe by the senior surgeon (JYKL) were taken. In addition to the 13 main tumor specimens, an additional 26 margin specimens were obtained. The number of margin biopsy specimens ranged from 1 to 4 with a median of 2 biopsies per patient.

We used NIR imaging to analyze the 13 main tumor samples with the 26 margin specimens (Table 3: Sensitivity and Specificity). Of the 39 specimens, 28 (71.8%) demonstrated metastases (tumor) tissue based on final histopathology and 35 (89.7%) were positive for NIR signal. The NIR SBR was higher in specimens positive for tumor by neuropathological determination than those which were negative. The mean SBR for the positive tumor specimens was 6.9 ± 1.5 whereas the SBR for the specimens which were negative for tumor by neuropathological diagnosis was 3.7 ± 1.4 (p value: < 0.001) (Figure 4: SBR for Positive vs Negative specimens). This was statistically significant difference using t-test (P<0.0005).

Using tumor on final pathology as the gold standard, the sensitivity, specificity, positive predictive value (PPV) and negative predictive value (NPV) based on the surgeon's

impression (visible light) alone were (respectively): 82.1%, 90.9%, 95.8%, 66.7%. In contrast, the sensitivity, specificity, PPV and NPV of NIR intraoperative imaging for identifying tumor was (respectively): 96.4%, 27.3%, 77.1%, and 75.0% (Table 3: Sensitivity and Specificity). Hence, NIR appeared to improve sensitivity at the expense of specificity. Note that the confidence intervals are very wide for the specificity of NIR, primarily because of the few number of samples. Of the eight samples with false-positive NIR signal, seven specimens demonstrated no specific pathologic change in normal brain, one specimen demonstrated necrosis, and none demonstrated inflammation or atypical cells.

Following surgery, 8 patients received gamma knife, 2 received cyber knife and 3 received no adjuvant radiotherapy. There were no adverse events due to the additional margin biopsies taken. 10 of the 13 patients (77%) had a gross total resection (Table 2: Near Infrared Signal of Gross Tumor Specimen). In the three patients without GTR, one patient had had prior Cyber Knife radiosurgery to seven metastasis in two separate settings spaced over a year. One of the metastasis progressed through radiosurgery, and the boundaries of the tumor and the scar were not abundantly clear intraoperatively. The majority of the pathologic specimen demonstrated necrosis, but “focal residual adenocarcinoma” was definitely identified in the pathology specimen (ID ICG23). Another patient had metastatic melanoma and similarly had prior Gamma Knife radiosurgery to a single melanoma metastasis which progressed through radiosurgery requiring surgical resection. The third patient had a bony clival metastasis from renal cell cancer which was causing a large nasopharyngeal mass causing dysphagia. The goal of the surgery was transoral/transnasal biopsy. Hence, the overall resection rate for intraparenchymal brain metastasis which had not been previously treated was 100%.

Higher camera gain percent for false positive specimens

The VisionSense Iridium™ camera system has a dynamic auto-exposure feature which averages the pixel intensity to normalize the background and then assigns it a neutral grey. The analogy to standard camera is when the camera is set on “auto-exposure”, the camera struggles to balance exposure between indoor lighting and outdoor sunlight for example. In bright sunlight, the camera exposes properly, and indoors the camera exposes properly. In the absence of NIR signal, the VisionSense™ system will boost exposure to find any NIR signal, and this tendency may be what is causing high false positive rate at the margins.

We analyzed the camera auto-gain percent for the true positive tumor specimens versus the false positive tumor specimens to further understand second window ICG in relation to the camera system. Post hoc analysis revealed the camera gain percent was 15.9% for the true positive tumor specimens (NIR positive and positive for tumor on pathology) and it climbed to 48.5% for the false positive specimens (NIR positive and negative for tumor on pathology) (Figure 5: Camera gain Percent for True Positive Specimens versus False Positive Specimens). This difference was not statistically significant using ttest (P=0.2913) or the Wilcoxon rank sum nonparametric test (P=0.1604). We suspect that allowing the gain to increase may lead to false positives, and thus the false positive rate may decrease if we lock the gain percentage at the same percentage as the TUMOR view.

In addition, we hypothesized that time from infusion until imaging could be a cause of the low specificity of second window ICG for tumor. The rates of false positive specimens (NIR positive and pathologically negative for tumor) did not increase with greater time from infusion.

Discussion

Although craniotomy for brain metastasis is associated with improved survival in patients with single brain metastasis, the local recurrence rate is a major source of mortality for patients and it can be quite high[24]. Patchell et al. demonstrate that after surgical resection of the metastasis, withholding radiation therapy results in a 46% chance of local recurrence in the surgical resection bed at one year[23]. As such, techniques for improved local control include radiosurgery[36] and brachytherapy[19,20]. We hypothesized that fluorescent-guided surgery may play a role in this effort, and as such we embarked on a pilot study to determine if intraoperative imaging with ICG could provide some relief to this devastating medical problem.

In this pilot study, 13 patients with brain metastases underwent a craniotomy after administration of an optical contrast near-infrared dye, using a technique we have labeled “Second Window ICG”. Indocyanine green has been used extensively by vascular neurosurgeons for well over a decade. ICG binds to plasma albumin and then is rapidly cleared from the circulation ($t_{1/2}$ < 10 minutes)[1]. In this study, however, we exploited the enhanced permeability and retention (EPR) effect to visualize ICG within brain metastasis at approximately 24 hours after intravenous infusion[1,6,7,9,15,17]. Because brain metastases disrupt the blood-brain barrier, ICG can leak into the tumor. Furthermore, since the tumor does not have a proper lymphatic system or clearance mechanism, the dye can remain in the tumor for many hours after serum clearance. A recent publication from our lab by Jiang et al. plots the time course of serum/tissue/tumor clearance in a rodent flank tumor model[9]. By administering ICG at 5 mg/kg, which is well below the LD_{50} for use in humans but a higher dose than what is usually administered during vascular neurosurgery, we were able to visualize NIR signal at several key points during the surgery. Prior to dural opening, the NIR camera can be used to localize the tumor, thus allowing for precise adjustments in dural incision. In addition, SWIG has potential for margin identification.

Prior Studies of Fluorescent-Guided Surgery for Brain Metastasis

Two most common contrast agents that have been used for intraoperative imaging of brain tumors are ICG and 5-ALA. Ferroli et al. reported on 12 patients with brain metastasis, and they describe the arterial, capillary and venous angiography views after a standard 25 mg ICG administered a few minutes prior to visualization[6]. Kim et al. reported on 3 patients with brain metastasis, and again the arterial, capillary and venous angiography are described after conventional 25 mg ICG intravenous bolus[11]. In both these publications, ICG was not used as a tumor optical contrast agent but rather as a vascular angiography technique.

The other studies use 5-ALA, a pro-drug that is enzymatically cleaved into a porphyrin which fluoresces in the visible light range. In Europe and Asia, 5-ALA has been studied as an optical contrast agent for brain metastasis resection. Kamp et al. administered

5-ALA to 52 patients who underwent surgery for brain metastasis[10]. 62% of the 52 patients demonstrated positive fluorescence, and the characterization of the fluorescence was described as heterogenous. The pattern of fluorescence did not appear to correlate with histology[10]. Similarly, Utsuki et al. administered 5-ALA to 11 patients, and 82% demonstrated positive fluorescence, but no pattern of non-fluorescence could be identified[33]. With respect to margin identification, Kamp et al. performed biopsy of residual fluorescence in 18 of the 52 patients, but only 6 were true positive for residual tumor resulting in a false positive rate of 66%, thus a specificity = 33%[10].

When we compare the SWIG technique to 5-ALA results in brain metastasis, we find that SWIG appears to be more reliable, in that all contrast-enhancing metastasis appear to accumulate dye[14]. In addition, SWIG appears to be more sensitive than 5-ALA (96% versus 62–82%), even though SWIG relies on passive accumulation of dye via a disrupted blood brain barrier, a proxy for which may be gadolinium enhancement on MRI scans. Despite the higher sensitivity, SWIG appears to suffer from low specificity. This limitation is quite similar to results with 5-ALA published by Kamp et al. where 5-ALA was only 33% specific in the margins SWIG is 27% specific in the margins[10].

Fluorescent-guided surgery has been reported in one paper with use of fluorescein, a visible light fluorescent dye used primarily for angiography. Okuda et al. reported the use of fluorescein but without use of a fluorescent filter, and as such the fluorescent properties of fluorescein were not exploited in this publication[22]. Nevertheless, by administering fluorescein as a simple intravenous dye, Okuda et al. reported that all 38 patients demonstrated positive yellow dye staining. Margins with residual tumor dye were not analyzed[22]. Compared to fluorescein, we believe that Second Window ICG provides more reliable tumor identification and possibly better margin detection.

Value of Second Window ICG technique for brain metastasis

In the current operating room environment, frameless and frame-based neuronavigational techniques are commonplace, and as such tumor localization is not necessarily a major hurdle. In this study, we used intraoperative navigational tools to plan the skin incision and the initial bone flap, as we could not see NIR signal through intact skull (unpublished results). Hence, SWIG cannot currently replace intraoperative navigation. However, once the dura is exposed, metastasis that are within a centimeter of the surface can be visualized with the dura intact (in this series up to 7mm)[13,14]. In some instances, we did find that the craniotomy was not centered over the tumor but was rather eccentric to one side or another, and as such, we were able to localize the dural opening more precisely using this technique. Hence, the longer wavelength of NIR did provide some technical value upon initial exposure.

Another benefit of SWIG for brain metastasis is that all 13 patients had a strong tumor NIR signal. Since all the brain metastasis did enhance with gadolinium, we hypothesized that gadolinium-enhancement may be a proxy for which tumors may accumulate ICG when administered at this high dose of 5mg/kg. We have previously published our work in gliomas where non-enhancing gliomas did not accumulate sufficient ICG to be visualized at the time of surgery, whereas all WHO grade I and grade IV gliomas did accumulate dye[14]. Thus, as

compared to 5-ALA and fluorescein, we believe the SWIG technique is more reliable as an optical contrast agent.

Potential sources of false positives with NIR imaging.

A critical role for any optical contrast tumor dye is the ability to assist the surgeon in the detection of margins that would go unnoticed to the naked eye. Despite the high sensitivity of SWIG for tumor, this technique suffers from low specificity. We have seen similar results in our work in gliomas[14]. Unfortunately, our technique suffered from a high rate of false positive specimens.

Although ICG is not a specific dye bound to a receptor in tumor cells, we considered that the false positive rate could be due to sex, age, prior surgery or radiation, tumor location, side and depth, and pre-op MRI findings including flair, mass effect and homogeneous gadolinium enhancement. In multivariate analysis, none of these factors predicted a false positive signal. We then postulated the false positive rate may be due to technical factors associated with either imaging technique or infusion time frame.

The NIR capable camera we used has an automatic exposure feature which either boosts or decreases the lens exposure in response to a weak or strong NIR signal, respectively. After analyzing this automatic gain percent, we learned that the true positive specimens had a gain percent of 15.9 whereas the false positive specimens had a gain percent of 48.5%. Allowing the gain percent to fluctuate in an automatic fashion may be the reason for the false positive margin specimens. Due to this fact, we have recently adjusted our imaging technique to lock the gain at the percentage seen when looking at the TUMOR view. As such, we do not see the gain percent climb during the MARGIN view and we believe this will ultimately reduce the number of false positive specimens.

We also hypothesized that time from infusion until imaging could be a cause of the low specificity of second window ICG for tumor. In a prior publication on meningiomas (in press), we identified time as a source of false positives at the margin, and as such we tested the hypothesis here. Unlike the meningioma subset, the rates of false positive specimens did not increase with greater time from infusion.

Additional factors not collected in this study may account for the false positive specimens. For example, because ICG is not bound to the tumor, excessive manipulation of the tumor during surgery may result in “spill”, and as such there may be confounders such as intratumor piecemeal resection versus en bloc resection.

Melanoma Brain Metastases displayed the weakest SBR

As can be seen in table 2, the two melanoma metastasis appeared to have the weakest SBR at 3.65 compared to the SBR of 7.2 for the other metastasis. We believe this may be in part due to melanin’s intrinsic property to block light penetration. As can be seen in figure 2, one patient had a hemorrhagic melanoma metastasis which was primarily cystic with an obscured mural nodule. Only after the cyst had been evacuated was the contrast-enhancing portion able to be viewed using fluorescence (Figure 2). The blood and melanin blocked the

NIR signal. This is in accordance with Ando et al. study which found melanin pigment to disrupt fluorescent staining of mitochondria in melanocytes[2].

Limitations of Second Window ICG

Indocyanine green binds to plasma albumin, and its mechanism of accumulation within tumors is not fully delineated. We suspect that ICG may aggregate at high concentrations and then act as a larger molecule which may exhibit properties that fall under the enhanced permeability and retention effect. Nevertheless, since ICG is not bound to a receptor, specific to the tumor, lack of specificity may be intrinsic to this technique. Nevertheless, we believe there are ways to mitigate the high false positive rate, specifically camera gain / auto-exposure as discussed above.

We acknowledge that there are several caveats to this study. First, this is a pilot study; therefore, the study size is small (n=13). In addition, SBR is an arbitrary number and may not a true measure of tissue fluorescence. Thus, correlating metabolism to fluorescence may not accurately represent the biology of the nodule. The test characteristics obtained in this study are largely determined by the number of biopsies taken at the time of surgery, and thus accurate test characteristic calculation is limited.

Conclusion

Second Window ICG is a technique of administration and visualization that relies on the enhanced permeability and retention of ICG in tumor tissue. This NIR optical contrast imaging technique provided strong signal to background ratio visualization of tumor tissue compared to surrounding brain, and it can provide imaging through normal dura and normal brain parenchyma. This allows the surgeon to see the tumor/dye even if the normal eye cannot. Its use for margin detection remains hampered by low specificity, but limiting auto-exposure may help to reduce false positives. In summary, the SWIG is a novel technique of visualization which can be easily applied by many practicing neurosurgeons.

Acknowledgements

This work was partially supported by the National Institutes of Health R01 CA193556 (SS), the Institute for Translational Medicine and Therapeutics of the Perelman School of Medicine at the University of Pennsylvania (JYKL), and National Center for Advancing Translational Sciences of the National Institutes of Health UL1TR000003 (JKYL). The content is solely the responsibility of the authors and does not necessarily represent the official views of the NIH.

Funding:

This work was partially supported by the National Institutes of Health R01 CA193556 (SS), Institute for Translational Medicine and Therapeutics of the Perelman School of Medicine at the University of Pennsylvania (JYKL), and National Center for Advancing Translational Sciences of the National Institutes of Health under Award Number UL1TR000003 (JKYL).

Abbreviations:

5-ALA	5-aminolevulinic acid
EPR	Enhanced Permeability and Retention

ICG	Indocyanine Green
MRI	Magnetic Resonance Imaging
ROI	Region-of-Interest
ROC	Receiver Operating Characteristic
SBR	Signal-to-Background Ratio
SWIG	Second Window ICG

References:

1. Alacam B, Yazici B, Intes X, Chance B: Analysis of ICG Pharmacokinetics in Cancerous Tumors using NIR Optical Methods. Conf Proc. Annu Int Conf IEEE Eng Med Biol Soc IEEE Eng Med Biol Soc Annu Conf 1:62–65, 2005
2. Ando H, Ohagi Y, Yoshida M, Yoshimoto S, Higashi Y, Yagi M, Uchiumi T, Kang D, Ichihashi M: Melanin pigment interupts the fluorescence staining of mitochondria in melanocytes. J Dermatol Sci (2016)
3. Coluccia D, Fandino J, Fujioka M, Cordovi S, Muroi C, Landolt H: Intraoperative 5-aminolevulinic-acid-induced fluorescence in meningiomas. Acta Neurochir (Wien) 152:1711–1719, 2010 [PubMed: 20535506]
4. Della Puppa A, Rustemi O, Gioffrè G, Troncon I, Lombardi G, Rolma G, et al. : Predictive value of intraoperative 5-aminolevulinic acid-induced fluorescence for detecting bone invasion in meningioma surgery. J Neurosurg 120:840–845, 2014 [PubMed: 24410157]
5. DSouza AV, Lin H, Henderson ER, Samkoe KS, Pogue BW: Review of fluorescence guided surgery systems: identification of key performance capabilities beyond indocyanine green imaging. J. Biomed. Opt 21(8), 080901, 2016 [PubMed: 27533438]
6. Ferroli P, Acerbi F, Albanese E, Tringali G, Broggi M, Franzini A, et al. : Application of intraoperative indocyanine green angiography for CNS tumors: results on the first 100 cases. Acta Neurochir Suppl 109:251–7, 2011 [PubMed: 20960352]
7. Greish K: Enhanced permeability and retention (EPR) effect for anticancer nanomedicine drug targeting. Methods Mol Biol 624:25–37, 2010 [PubMed: 20217587]
8. Holt D, Okusanya O, Judy R, Venegas O, Jiang J, DeJesus E, et al. : Intraoperative near-infrared imaging can distinguish cancer from normal tissue but not inflammation. PLoS One 9:2014
9. Jiang JX, Keating JJ, Jesus EM, Judy RP, Madajewski B, Venegas O, et al. : Optimization of the enhanced permeability and retention effect for near-infrared imaging of solid tumors with indocyanine green. Am J Nucl Med Mol Imaging. 4:390–400, 2015
10. Kamp MA, Grosser P, Felsberg J, Slotty PJ, Steiger HJ, Reifenberg G, Sabel M: 5-Aminolevulinic acid (5-ALA)-induced fluorescence in intracerebral metastases: a retrospective study. Acta Neurochir (2012) 154:223–228 [PubMed: 22080159]
11. Kim EH, Cho JM, Chang JH, Kim SH, Lee KS: Application of intraoperative indocyanine green videoangiography to brain tumor surgery. Acta Neurochir (Wien) 153:1487–1495; discussion 1494–5, 2011 [PubMed: 21590519]
12. Kubben PL, ter Meulen KJ, Schijns OE, ter Laak-Poort MP, van Overbeeke JJ, Santbrink H van: Intraoperative MRI-guided resection of glioblastoma multiforme: a systematic review. Lancet Oncol 12:1062–1070, 2011 [PubMed: 21868286]
13. Lee JYK, Pierce JT, Thawani JP, Zeh R, Nie S, Martinez-Lage M, Singhal S: Near-Infrared Fluorescent Dye Provides Optical Contrast During Surgery of Intracranial Meningiomas. In press
14. Lee JYK, Thawani JP, Pierce JT, Zeh R, Martinez-Lage M, Chanin M, Venegas O, Nims S, Keating J, Singhal S: Intraoperative Near-Infrared Optical Imaging Can Localize Gadolinium-Enhancing Gliomas During Surgery. In press

15. Maeda H, Greish K, Fang J: The EPR effect and polymeric drugs: A paradigm shift for cancer chemotherapy in the 21st century. Adv Polym Sci 193:103–121, 2006
16. Maeda H, Tsukigawa K, Fang J: A Retrospective 30 Years After Discovery of the Enhanced Permeability and Retention Effect of Solid Tumors: Next-Generation Chemotherapeutics and Photodynamic Therapy-Problems, Solutions, and Prospects. Microcirculation. 3:173–182, 2016
17. Maeda H, Wu J, Sawa T, Matsumura Y, Hori K: Tumor vascular permeability and the EPR effect in macromolecular therapeutics: a review. J Control Release 65:271–284, 2000 [PubMed: 10699287]
18. Marshall MV, Rasmussen JC, Tan I-C, Aldrich MB, Adams KE, Wang X, et al. : Near-Infrared Fluorescence Imaging in Humans with Indocyanine Green: A Review and Update. Open Surg Oncol J 2:12–25, 2010 [PubMed: 22924087]
19. Matsumura Y, Maeda H: A new concept for macromolecular therapeutics in cancer chemotherapy: Mechanism of tumoritropic accumulation of proteins and the antitumor agent smancs. Cancer Res 46:6387–6392, 1986 [PubMed: 2946403]
20. Mu F, Lucas JT, Watts JM, Johnson AJ, Bourland JD, Laxton AW, Chan MD, Tatter SB: Tumor resection with carmustine wafer placement as salvage therapy after local failure of radiosurgery for brain metastasis. Journal of Clinical Neuroscience: 22 (2015) 561–565 [PubMed: 25560387]
21. Nussbaum ES, Djalilian HR, Cho KH, Hall WA: Brain metastases. Histology, multiplicity, surgery, and survival. Cancer: 1996 Oct 15;78(8): 1781–1788 [PubMed: 8859192]
22. Okuda T, Kataoka K, Yabuuchi T, Yugami H, Kato A: Fluorescence-guided surgery of metastatic brain tumors using fluorescein sodium. Journal of Clinical Neuroscience. 17 (2010) 118–121 [PubMed: 19969462]
23. Patchell RA, Tibbs PA, Regine WF, Dempsey RJ, Mohiuddin M, Kryscio RJ, Markesbery WR, Foon KA, Young B: Postoperative Radiotherapy in the Treatment of Single Metastases to the Brain: A Randomized Trial. JAMA 1998;280:1485–1489 [PubMed: 9809728]
24. Patchell RA, Tibbs PA, Walsh JW, Dempsey RJ, Maruyama Y, Kryscio RJ, Markesbery WR, Macdonald JS, Young B: A Randomized Trial of Surgery in the Treatment of Single Metastases to the Brain. N Engl J Med 1990: 322:494–500. [PubMed: 2405271]
25. Pogue BW, Gibbs-Strauss SL, Valdés PA, Samkoe KS, Roberts DW, Paulsen KD: Review of Neurosurgical Fluorescence Imaging Methodologies. IEEE J Sel Top Quantum Electron 16:2010
26. Predina J, Eruslanov E, Judy B, Kapoor V, Cheng G, Wang L-C, et al. : Changes in the local tumor microenvironment in recurrent cancers may explain the failure of vaccines after surgery. Proc Natl Acad Sci U S A 110:E415–424, 2013 [PubMed: 23271806]
27. Puppa A Della, Rustemi O, Gioffrè G: Application of indocyanine green video angiography in parasagittal meningioma surgery. Neurosurg … 36:1–8, 2014
28. Scerrati a, Della Pepa GM, Conforti G, Sabatino G, Puca a, Albanese a, et al. : Indocyanine green video-angiography in neurosurgery: a glance beyond vascular applications. Clin Neurol Neurosurg 124:106–113, 2014 [PubMed: 25033322]
29. Singhal S, Holt D, Nie S, Wang MD, Madajewski B, Judy BF, et al. : Intraoperative Near-Infrared Imaging of Surgical Wounds after Tumor Resections Can Detect Residual Disease. Clin Cancer Res 18:5741–5751, 2012 [PubMed: 22932668]
30. Singhal S, Nie S, Wang MD: Nanotechnology applications in surgical oncology. Annu Rev Med 61:359–373, 2010 [PubMed: 20059343]
31. Stummer W, Pichlmeier U, Meinel T, Wiestler OD, Zanella F, Reulen H-J: Fluorescence-guided surgery with 5-aminolevulinic acid for resection of malignant glioma: a randomised controlled multicentre phase III trial. Lancet Oncol 7:392–401, 2006 [PubMed: 16648043]
32. Stummer W, Novotny A, Stepp H, Goetz C, Bise K, Reulen HJ: Fluorescence-guided resection of glioblastoma multiforme by using 5-aminolevulinic acid-induced porphyrins: a prospective study in 52 consecutive patients. J Neurosurg 93:1003–1013, 2000 [PubMed: 11117842]
33. Utuski S, Miyoshi N, Oka H, Miyajima Y, Shimizu S, Suzuki S, Fujii K: Fluorescence-guided resection of metastatic brain tumors using a 5-aminolevulinic acid-induced protoporphyrin IX: pathological study. Brain Tumor Pathol (2007) 24:53–55 [PubMed: 18095131]
34. Valdes P a, Bekelis K, Harris BT, Wilson BC, Leblond F, Kim A, et al. : 5-Aminolevulinic acid-induced protoporphyrin IX fluorescence in meningioma: qualitative and quantitative measurements in vivo. Neurosurgery 10 Suppl 1:74–82; discussion 82–38, 2014 [PubMed: 23887194]

35. Valdés PA, Leblond F, Kim A, Harris BT, Wilson BC, Fan X, et al. : Quantitative fluorescence in intracranial tumor: implications for ALA-induced PpIX as an intraoperative biomarker. J Neurosurg 115:11–17, 2011 [PubMed: 21438658]

36. Vogel J, Ojerholm E, Hollander A, Briola C, Mooij B, Bieda M, et al. : Intracranial control after Cyberknife radiosurgery to the resection bed for large brain metastases. Radiation Oncology (2015) 10:221 [PubMed: 26520568]

37. Zhao S, Wu J, Wang C, Liu H, Dong X, Shi C, et al. : Intraoperative Fluorescence-Guided Resection of High-Grade Malignant Gliomas Using 5-Aminolevulinic Acid-Induced Porphyrins: A Systematic Review and Meta-Analysis of Prospective Studies. PLoS One 8:2013

Highlights

- Our lab has pioneered a novel technique, “Second Window Indocyanine Green (SWIG)”
- Allows for intraoperative visualization of brain metastasis through normal brain parenchyma and intact dura.
- Relies on the passive accumulation of dye in abnormal tumor tissue via the enhanced permeability and retention (EPR) effect.
- Provides strong NIR SBR ratio which can be utilized to localize tumors prior to dural opening
- May aid in identifying residual disease

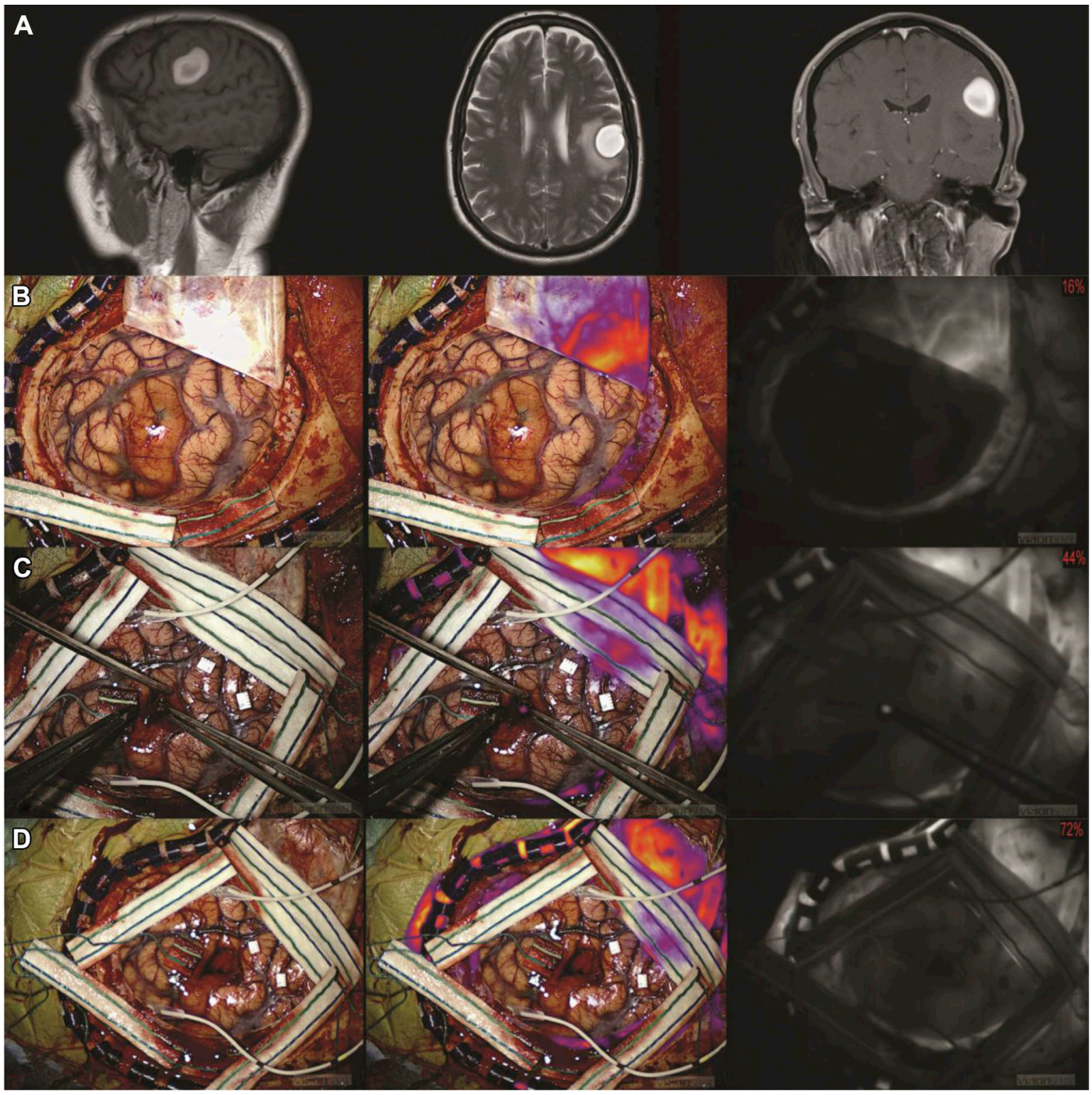

Figure 1: Intraoperative NIR view of Patient with Lung Cancer Metastasis to Brain.

Each vertical column displays a type of imaging performed by the camera system. The first left column displays the visible light image only, the middle column displays the NIR image fused over a visible light image and the third right column displays the near infrared only image. Horizontal row (A) displays the preoperative MRI images showing a right temporal/occipital metastasis that does is just below the cortex. Row (B) displays the imaging seen with the dura intact and not yet opened – DURA view. NIR signal can be seen localizing just under the dura at the presumed location of the tumor. Row (C) displays the images after the dura is opened but prior to corticectomy – CORTEX view. Even though the tumor cannot be seen with visible light alone because of overlying brain parenchyma, the tumor can be seen using the NIR camera system. Row (D) displays the tumor after corticectomy and as it is being resected TUMOR view.

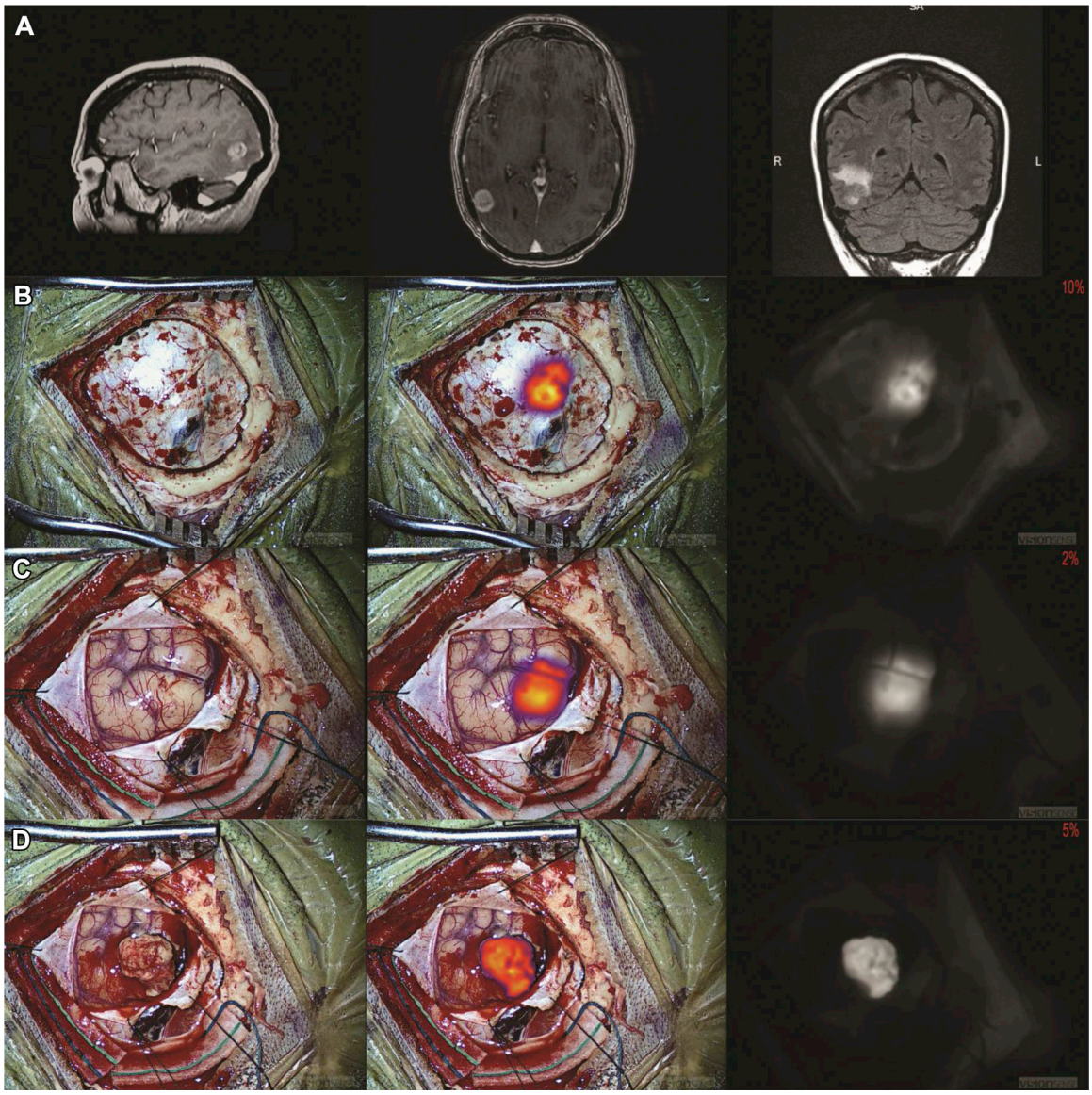

Figure 2: Intraoperative NIR view of patient with Melanoma Metastasis to Brain.

Each vertical column displays a type of imaging performed by the camera system. The first left column displays the visible light image only, the middle column displays the NIR image fused over a visible light image and the third right column displays the near infrared only image. Horizontal row (A) displays the preoperative MRI images. Row (B) displays the image after the dura has been opened – CORTEX view. There is nonspecific fluorescence in skin and dura. Notably, however, the cystic portion of the melanoma does not contain any NIR dye signal. Only upon evacuation of the cystic melanotic hemorrhagic contents is the mural nodule/melanoma metastasis identified which is sent to pathology for confirmation of melanoma. See deep cavity. Row (C) displays the margin view after the main tumor was resected and a NIR positive nodule can be seen which was biopsied. Row (D) displays the final margin view which demonstrates no residual NIR signal in the cavity which is ultimately correlated with complete resection on MRI scan.

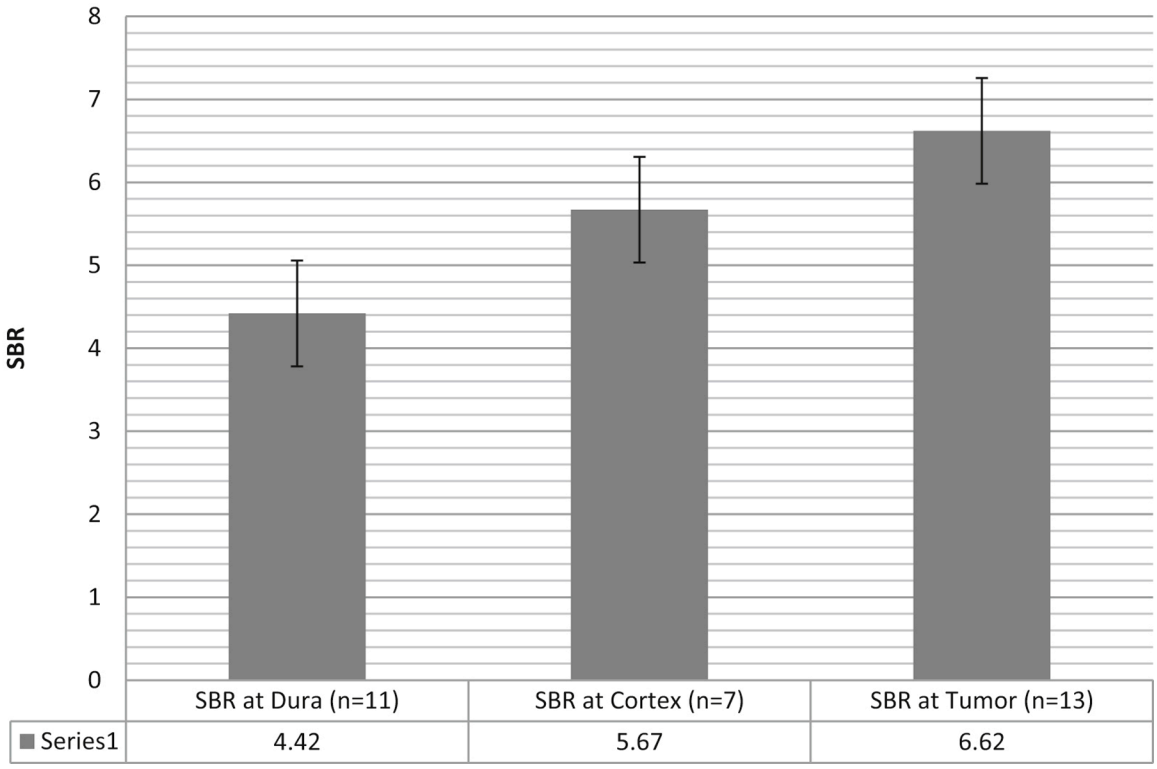

Figure 3: NIR Signal to background ratio at different depths.

The NIR signal is smaller above the dura and above the cortex, but it is still visible even despite dura covering the tumor. NIR signal to background ratio at Dura view, Cortex view, and Tumor view. Error bars represent that standard error of the mean. The ANOVA test for multiple groups demonstrated a trend towards a statistically significant difference between the three groups (P=0.2126).

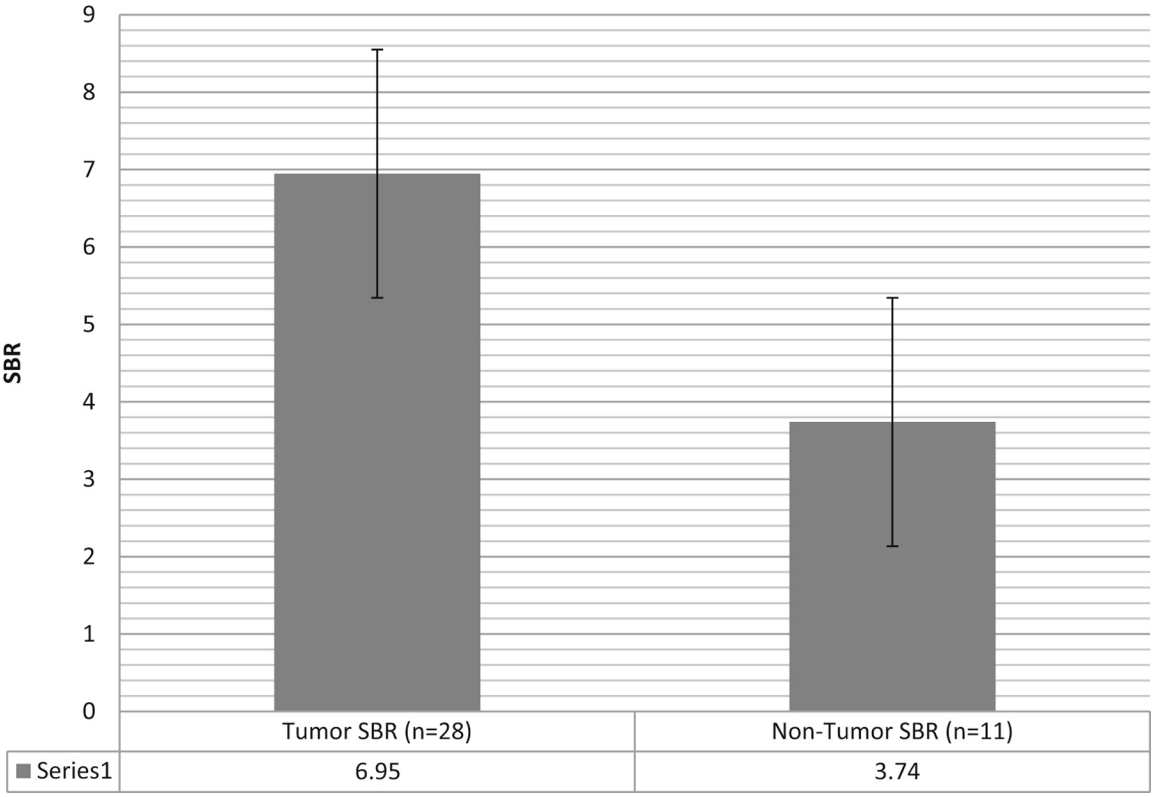

Figure 4: NIR signal of pathology positive tumor versus nontumor specimens.

Signal-to-background ratio for the specimens histopathologically positive for tumor versus those histopathologically negative for tumor determined by neuropathology. Error bars represent that standard error..T test comparison demonstrates statistically significant difference between two groups (P<0.0005).

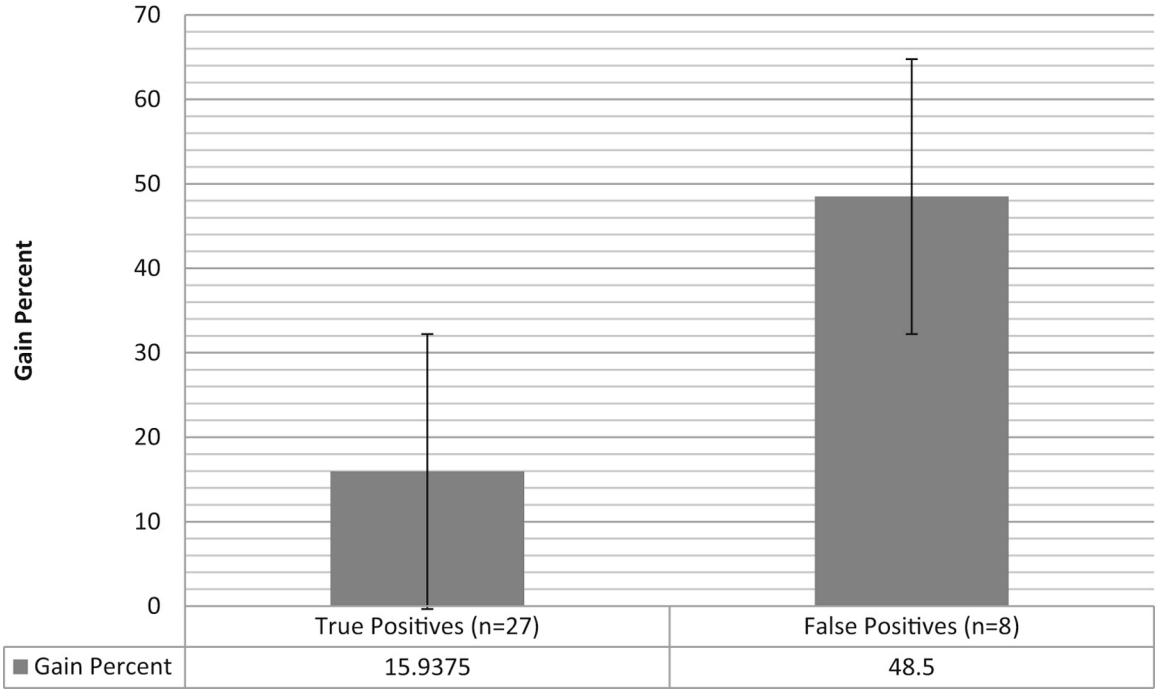

Figure 5: Camera Gain Percentage may be source of variability in signal.

The 27 true positive samples had camera gain percentage average of 15.9. The 8 false positive samples had camera gain percentage average of 48.5. Because of the few number of samples, we tested difference using Wilcoxon rank sum nonparametric (P=0.1604) which does not quite reach significance.

Table 1.

Description of Patients: Demographics and Injection Parameters

Final Pathology	ID	Age (years)	Gender	Location	Tumor Volume (mm^3)	ICG Injection Dose (mg)	Patient Weight (kg)	Time from ICG Injection to Camera Visualization (hours)	Previous Surgery or Radiation	Months Since Last Intervention
Lung	ICG 16	48	F	Right temporal	526	343	68.5	27.0		
	ICG 23	63	F	Left parietal occipital	194	388.5	77.3	25.8		
	ICG 3S	58	F	Right parietal	3344	397	78.9	27.5		
	ICG 19S	65	M	Left parietal	2549	397	79.4	19.9		
Melanoma	ICG 04	59	M	Left frontal	1242	476.5	95.3	21.0		
	ICG 27	60	F	Right temporal	456	316	63.1	28.6	Radiation	31
Breast	ICG 41	73	F	Left parietal	4586	457	91.4	21.9		
	ICG 4S	50	F	Left cerebellar		327.5	63.5	26.6		
Colon	ICG 26	71	F	Right occipital	13974	256.5	51.2	19.9	Radiation and surgery	3, 4
	ICG 45	36	F	Right frontal	6879	258.5	21.5	26.7		
Other										
Ovarian	ICG 14	58	F	Right parietal	3151	317.5	63.5	27.3	Radiation and surgery	10, 40
Kidney	ICG 36	64	M	Cerebellopontine angle	7797	72.6	93.4	20.8		
Esophageal	ICG 30	64	M	Right temporal	1299	300.5	39.9	28.7		

ICG, indocyanine green; F, female; M, male.

Table 2.

Near-Infrared Signal of Gross Tumor Specimen

Pathology	ID	Maximum Diameter (mm) on Preoperative MRI	Gadolinium Enhancement on MRI	Signal Visible with Near-Infrared Camera	T1 Tumor-to-Nontumor Signal Ratio	Signal-to-Background Ratio	Gross Total Resection
Lung	ICG 16	20	Yes	Yes	1.7	7.0	Yes
	ICG 23	16.5	Yes	Yes	2.2	7.7	No
	ICG 3S	22	Yes	Yes	1.6	6.7	Yes
	ICG 19S	18.5	Yes	Yes	2.0	7.7	Yes
Melanoma	ICG 04	25.3	Yes	Yes	2.1	4.3	Yes
	ICG 27	22.7	Yes	Yes	1.5	3.0	No
Breast	ICG 41	31.2	Yes	Yes	2.6	6.9	Yes
	ICG 4S	25	Yes	Yes	2.2	8.1	Yes
Colon	ICG 26	16.1	Yes	Yes	2.4	6.9	Yes
	ICG 45	44.3	Yes	Yes	1.9	5.8	Yes
Other							
Ovarian	ICG 14	36.6	Yes	Yes	1.5	8.7	Yes
Kidney	ICG 36	28.2	Yes	Yes	1.7	6.1	No
Esophageal	ICG 30	29.1	Yes	Yes	1.2	7.2	Yes

MRI, magnetic resonance imaging; ICG, indocyanine green.

Table 3.

Sensitivity and Specificity

White Light vs. Pathology	White Light			Sensitivity	Specificity	Positive Predictive Value	Negative Predictive Value	Receiver Operating Characteristic Area
	Pos	Neg						
Pathology								
Pos	23	5	Point estimate	82.1	90.9	95.8	66.7	0.865
Neg	1	10	95% CI	63.1–93.9	58.7–99.8	78.9–99.9	38.4–88.2	0.734–0.996
	Total n	39						
	Near-Infrared							
NIR vs. Pathology	Pos	Neg						
Pathology								
Pos	27	1	Point estimate	96.4	27.3	77.1	75	0.619
Neg	8	3	95% CI	81.7–99.9	6.0–61	59.9–89.6	19.4–99.4	0.406–0.831
	Total n	39						

Pos, positive; Neg, negative; CI, confidence interval.